
DESIGN OPTIMISATION OF A MULTI-MODE WAVE ENERGY CONVERTER

A PREPRINT

Nataliia Y. Sergiienko

School of Mechanical Engineering
The University of Adelaide
Australia
nataliia.sergiienko@adelaide.edu.au

Mehdi Neshat

Optimization and Logistics Group
School of Computer Science
The University of Adelaide
Australia
mehdi.neshat@adelaide.edu.au

Leandro S.P. da Silva

School of Mechanical Engineering
The University of Adelaide
Australia
leandro.dasilva@adelaide.edu.au

Bradley Alexander

Optimization and Logistics Group
School of Computer Science
The University of Adelaide
Australia
bradley.alexander@adelaide.edu.au

Markus Wagner

Optimization and Logistics Group
School of Computer Science
The University of Adelaide
Australia
markus.wagner@adelaide.edu.au

January 27, 2020

ABSTRACT

A wave energy converter (WEC) similar to the CETO system developed by Carnegie Clean Energy is considered for design optimisation. This WEC is able to absorb power from heave, surge and pitch motion modes, making the optimisation problem nontrivial. The WEC dynamics is simulated using the spectral-domain model taking into account hydrodynamic forces, viscous drag, and power take-off forces. The design parameters for optimisation include the buoy radius, buoy height, tether inclination angles, and control variables (damping and stiffness). The WEC design is optimised for the wave climate at Albany test site in Western Australia considering unidirectional irregular waves. Two objective functions are considered: (i) maximisation of the annual average power output, and (ii) minimisation of the levelised cost of energy (LCoE) for a given sea site. The LCoE calculation is approximated as a ratio of the produced energy to the significant mass of the system that includes the mass of the buoy and anchor system. Six different heuristic optimisation methods are applied in order to evaluate and compare the performance of the best known evolutionary algorithms, a swarm

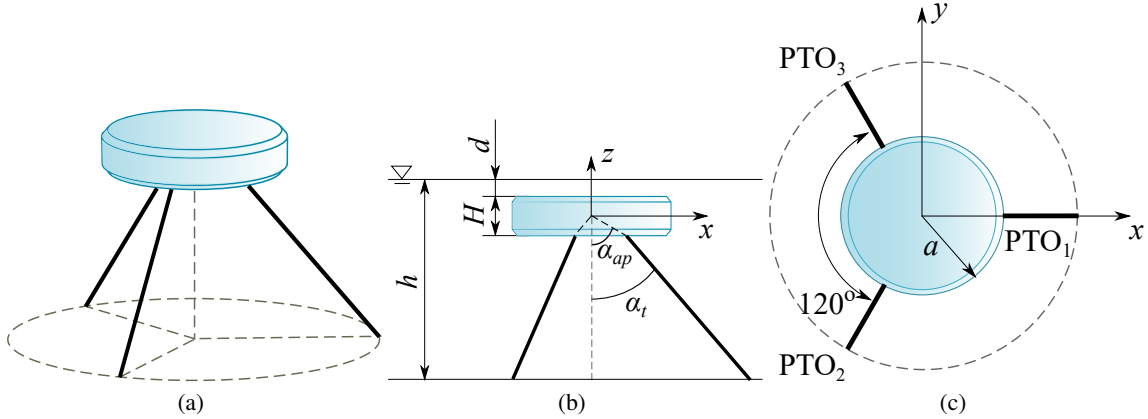


Figure 1: Geometry and parameters of the three-tether wave energy converter: (a) 3D view, (b) front view, (c) top view.

intelligence technique and a numerical optimisation approach. The results demonstrate that if we are interested in maximising energy production without taking into account the cost of manufacturing such a system, the buoy should be built as large as possible (20 m radius and 30 m height). However, if we want the system that produces cheap energy, then the radius of the buoy should be approximately 11-14 m while the height should be as low as possible. These results coincide with the overall design that Carnegie Clean Energy has selected for its CETO 6 multi-moored unit. However, it should be noted that this study is not informed by them, so this can be seen as an independent validation of the design choices.

Keywords Renewable Energy · Design Optimisation · Multi-Mode Wave Energy Converters · Power Take Off system, Evolutionary Algorithms.

1 Introduction

The geometry of a wave energy converter (i.e., its shape and size) determines how efficiently it radiates waves and absorbs incident wave power. A number of studies have been conducted to develop recommendations for wave energy developers regarding the hydrodynamic design of WECs [1, 2]. In the latter, the optimal dimensions of the wave absorbing body are chosen from the point of view of maximising power production, and depending on the mode of oscillation (heave, surge, or pitch) [3] and applied control strategy [4]. Similarly, the annual power output has been used as an objective function for shape optimisation of various WECs in [5, 6, 7, 8].

However, the economic attractiveness of any wave energy project depends not only on its power production, but also on the costs associated with a project lifetime [9]. Therefore, the economic component should be integrated into the WEC design to make wave energy cost-effective. Despite the fact that the levelised cost of energy is the most reliable metric to assess energy investments, its calculations for wave energy devices are full of assumptions and uncertainties. Therefore, other cost-related measures have been widely used for techno-economic development of WECs. Thus,

power per displaced volume of the buoy was utilised in [10] to optimise the shape of a surging WEC for a site in the North-East Atlantic Ocean. As the optimised shapes were complex and not adequate for construction, the research has been extended in [11] by including the cost of materials and manufacturing processes into the optimisation procedure. In addition to the costs associated with a buoy construction, [12, 13] suggest taking into account the PTO-reliability at the early stages of the WEC hull optimisation.

The majority of geometry optimisation studies consider WECs that absorb power from one hydrodynamic mode (e.g. heave [7], surge [14], or pitch [6]). This work focuses on the CETO 6 technology being under development by Carnegie Clean Energy Limited, Australia. The CETO 6 design was announced in 2017 and consists of a submerged cylindrical buoy (25 m diameter) attached to three mooring lines capturing power from heave, surge and pitch motions. The first attempts to understand how the dimensions of a submerged cylindrical buoy (radius and height) affect its power efficiency depending on the motion mode has been made in [15]. However, only a number of prescribed geometries were investigated without a properly designed optimisation procedure. As a result, this paper addresses three main objectives:

- (i) to optimise the geometry of a WEC that absorbs power from surge, heave and pitch simultaneously;
- (ii) to investigate how this geometry depends on the chosen objective function: power production, or LCoE;
- (iii) to understand the design solution for CETO 6.

MODELLING

Wave energy converter

The wave energy converter considered in this work is shown in Fig. 1. A fully submerged cylindrical buoy is tied to the seabed through three tethers. It is assumed that each tether is connected to an individual power take-off (PTO) machinery that is capable to behave as a spring-damper system. The parameters that define the size of the cylinder are radius (a), and height (H). The buoy is designed to operate at $d = 2$ m below the water surface (from the buoy top to the still water level), in the water column of $h = 50$ m. The attachment of tethers to the buoy hull is defined by two distinct angles: the tether inclination angle (α_t), and the tether attachment angle, or attachment point, (α_{ap}). The mass of the buoy is equal to half the displaced mass of water $m_b = 0.5\rho_w V$ ($\rho_w = 1025$ kg/m³, and $V = \pi a^2 H$).

This WEC will be installed at the so-called Albany test site in Western Australia, which has a wave climate specified in Fig. 2. In order to reduce the number of sea states considered to assess the WEC performance, a sub-set of 34 sea states with a total probability of 99% are chosen to represent the deployment climate (outlined by a black line).

Time-domain model

A detailed description of the non-linear time domain model of the three-tether WEC has been documented in [17, 18, 19] and only key points are outlined in the following.

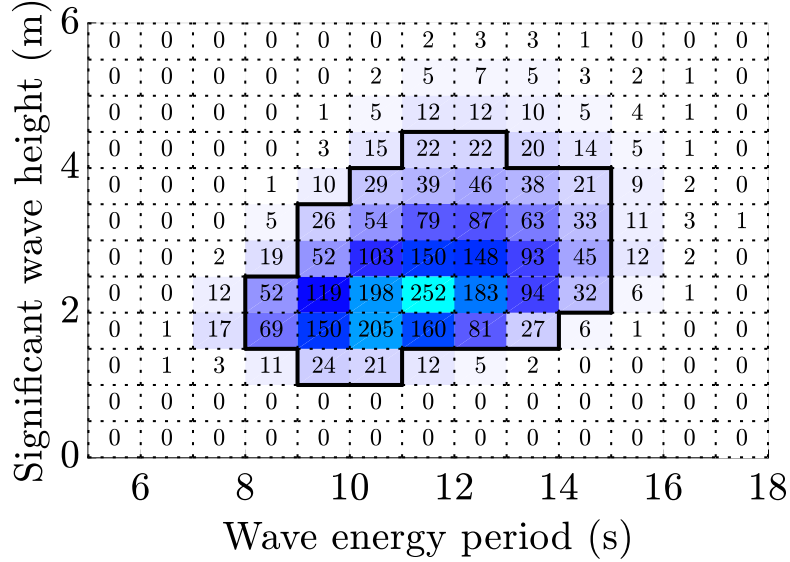


Figure 2: The wave climate at the Albany deployment site located in Western Australia (117.7547°E, 35.1081°S, 33.9 kW/m mean annual wave power resource) [16].

The WEC has six degrees-of-freedom, and its motion is described by the position vector $\mathbf{x} \in \mathbb{R}^{6 \times 1}$ (x_1 surge, x_2 sway, x_3 heave, x_4 roll, x_5 pitch, x_6 yaw) in the reference (Cartesian) coordinate frame $Oxyz$. The buoy is connected to three tethers that are represented by the vector of tether length variables $\mathbf{q} = [l_1 \ l_2 \ l_3]^T$. The kinematic relationship between the buoy velocity $\dot{\mathbf{x}}$ and the rate of change of the tether length has a form of $\dot{\mathbf{q}}(t) = \mathbf{J}^{-1}(\mathbf{x})\dot{\mathbf{x}}(t)$, where $\mathbf{J}^{-1}(\mathbf{x}) \in \mathbb{R}^{3 \times 6}$ is the inverse kinematic Jacobian which is a function of the buoy current pose [15].

The motion of the three-tether WEC in the time domain can be described by the following equation:

$$\mathbf{M}\ddot{\mathbf{x}}(t) = \mathbf{F}_{exc}(t) + \mathbf{F}_{rad}(t) + \mathbf{F}_{visc}(t) + \mathbf{F}_{buoy}(t) + \mathbf{F}_{tens}(t), \quad (1)$$

where \mathbf{M} is a mass matrix, \mathbf{F}_{exc} is the wave excitation force, \mathbf{F}_{rad} is the wave radiation force, \mathbf{F}_{visc} is the viscous damping force, \mathbf{F}_{buoy} is the buoyancy force, \mathbf{F}_{tens} is the generalised tether force which includes the initial tension in the tethers that counteracts the buoyancy force, and the control forces exerted on the buoy from the PTO machinery.

As optimisation procedures typically require a large number of evaluations to be performed in order to find the best WEC configuration for a given objective function, a low computational cost is desired: the lower the computational cost of the model, the faster the optimisation algorithm converges in terms of wallclock time. Therefore, in order to develop the computationally efficient model suitable for optimisation purposes, the nonlinear Eq. (1) is replaced by its linear equivalent spectral-domain model using the statistical linearisation technique.

Spectral-domain model

The spectral-domain model of the system is a set of linear equations of motion written in the frequency domain that approximates the system dynamics by replacing all nonlinear terms with their linear counterparts [20]. For the

proposed three-tether device, the main source of nonlinearity comes from the viscous drag force, while the geometric nonlinearity from the tethers can be linearised around the equilibrium position. Thus, assuming a harmonic response of the WEC $\mathbf{x}(t) = \Re\{\hat{\mathbf{x}} e^{i\omega t}\}$, the equivalent linear system for the nonlinear Eq. (1) in the frequency domain has a form:

$$[-\omega^2 (\mathbf{M} + \mathbf{A}) + i\omega (\mathbf{B} + \mathbf{B}_{pto} + \mathbf{B}_{eq}) + \mathbf{K}_{pto}] \hat{\mathbf{x}}(\omega) = \hat{\mathbf{F}}_{exc}(\omega) \quad (2)$$

where $\mathbf{A}(\omega)$ and $\mathbf{B}(\omega)$ are the frequency dependent added mass and radiation damping matrices, \mathbf{K}_{pto} and \mathbf{B}_{pto} are obtained from the linearisation of the generalised tether force $\hat{\mathbf{F}}_{tens}(\omega) = -\mathbf{B}_{pto}\hat{\mathbf{x}}(\omega) - \mathbf{K}_{pto}\hat{\mathbf{x}}(\omega)$ (see [17] for more details), and \mathbf{B}_{eq} is the equivalent damping matrix that corresponds to the quadratic damping nonlinearity. The value of \mathbf{B}_{eq} is unknown and can be determined iteratively using the statistical linearisation [21]:

$$\mathbf{B}_{eq} = -\left\langle \frac{\partial \mathbf{F}_{visc}}{\partial \dot{\mathbf{x}}} \right\rangle, \quad (3)$$

where $\langle \cdot \rangle$ denotes mathematical expectation, and the viscous force is defined as:

$$\mathbf{F}_{visc} = -\frac{1}{2}\rho_w \mathbf{C}_d \mathbf{A}_d (|\dot{\mathbf{x}}| \odot \dot{\mathbf{x}}), \quad (4)$$

\mathbf{C}_d and \mathbf{A}_d are the matrices of the drag coefficients and the cross-section areas of the buoy perpendicular to the direction of motion respectively.

To calculate \mathbf{B}_{eq} and estimate the approximate response of the WEC in irregular waves, the following iterative procedure is employed:

Step 1. Define the incident wave spectrum $S_\eta(\omega)$

Step 2. Calculate the power spectral density (PSD) matrix of the excitation force:

$$\mathbf{S}_F(\omega) = S_\eta(\omega) \cdot \text{diag}(|\hat{f}_{exc,1}|^2, \dots, |\hat{f}_{exc,6}|^2) \quad (5)$$

where $\hat{f}_{exc,i}(\omega)$ is the frequency-dependent excitation force coefficient for the i -th degree of freedom.

Step 3. Obtain the frequency response matrix of the WEC:

$$\mathbf{H}(\omega) = [-\omega^2 (\mathbf{M} + \mathbf{A}) + i\omega (\mathbf{B} + \mathbf{B}_{pto} + \mathbf{B}_{eq}) + \mathbf{K}_{pto}]^{-1} \quad (6)$$

assuming $\mathbf{B}_{eq} = \mathbf{0}_{6 \times 6}$ in the first iteration.

Step 4. Determine the PSD matrix of the buoy response:

$$\mathbf{S}_x(\omega) = \mathbf{H}(\omega) \mathbf{S}_F(\omega) \mathbf{H}^{T*}(\omega). \quad (7)$$

Step 5. Calculate the variance of the WEC velocity in each degree of freedom $i = 1 \dots 6$:

$$\sigma_{\dot{x}_i}^2 = \int_0^\infty \omega^2 S_{x_i}(\omega) d\omega \quad (8)$$

Step 6. Estimate the equivalent damping matrix $\mathbf{B}_{eq} = \text{diag}(B_{eq,1}, \dots, B_{eq,6})$, where according to [21]:

$$B_{eq_i} = - \left\langle \frac{\partial F_{visc_i}}{\partial \dot{x}_i} \right\rangle = \frac{1}{2} \rho_w C_{d_i} A_{d_i} \sqrt{\frac{8}{\pi}} \sigma_{\dot{x}_i} \quad (9)$$

Step 7. Check the convergence criteria: the difference between all elements of \mathbf{B}_{eq} obtained in the current $[n]$ and previous $[n - 1]$ iterations should be less than a threshold $\delta = 0.01$:

$$|\mathbf{B}_{eq}[n] - \mathbf{B}_{eq}[n - 1]| < \delta. \quad (10)$$

If the convergence is not achieved, go to Step 3.

It usually takes up to 10 iterations to find the equivalent damping matrix \mathbf{B}_{eq} for any WEC geometry operating in one sea state.

The average power output from each of the three power take-off units $k = 1 \dots 3$ can be found as [21]:

$$\bar{P}_k = B_{pto} \sigma_{\dot{q}_k}^2, \quad (11)$$

where $\sigma_{\dot{q}_k}^2$ is the variance of the tether length rate change $\dot{\mathbf{q}}$ that can be calculated as:

$$\sigma_{\dot{q}_k}^2 = \int_0^\infty \omega^2 S_{q_k}(\omega) d\omega, \quad (12)$$

where $\mathbf{S}_q(\omega) = \mathbf{J}_0^{-1} \mathbf{S}_x(\omega) \mathbf{J}_0^{-T}$, and $\mathbf{J}_0^{-1} = \mathbf{J}^{-1}(\mathbf{x}_0)$ is the inverse kinematic Jacobian at the nominal position of the buoy $\mathbf{x}_0 = \mathbf{0}_{6 \times 1}$.

Thus, the power generated by the WEC in a sea state characterised by the significant wave height H_s and peak wave period T_p is:

$$\bar{P}(H_s, T_p) = B_{pto} \sum_{k=1}^3 \sigma_{\dot{q}_k}^2(H_s, T_p). \quad (13)$$

If the probability of occurrence of each sea state (H_s, T_p) is characterised by the matrix $\mathbf{O}(H_s, T_p)$, then the total average annual power output generated by the WEC in the wave climate can be calculated as:

$$P_{AAP} = \sum_{H_s} \sum_{T_p} \mathbf{O}(H_s, T_p) \cdot \bar{P}(H_s, T_p). \quad (14)$$

To demonstrate the effectiveness of the spectral-domain model, the average output power of the three-tether WEC is shown in Fig. 3 using three different models (frequency, spectral, and time domain). As expected, the frequency domain model (Eq. (2) assuming $\mathbf{B}_{eq} = \mathbf{0}$) significantly overestimates the absorbed power. The time domain and spectral domain models provide similar estimates of power output, while the latter is approximately several orders of magnitude faster.

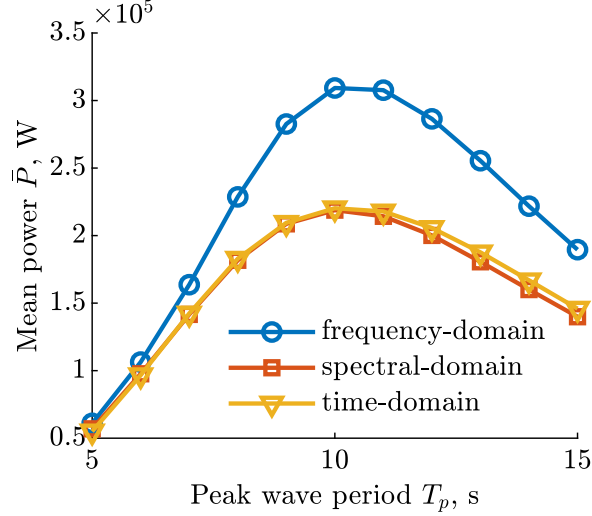


Figure 3: Average power output of the three-tether WEC ($a = 5.5$ m, $H = 5.5$ m, $\alpha_{ap} = \alpha_t = 45$ deg, $K_{pto} = 200$ kN/m, $B_{pto} = 150$ kN/(m/s)) calculated using frequency-, time- and spectral domain models. All sea states have the significant wave height of $H_s = 3$ m and are described by the Pierson-Moskowitz spectrum.

The values of the viscous drag force and, consequently, the values of the linearised \mathbf{B}_{eq} matrix depend on the drag coefficients C_{d_i} ($i = 1 \dots 6$) taken for the analysis. C_{d_i} depends on the ratio of the cylinder length (or height) to its diameter, especially for the heave direction $i = 3$. Therefore, for optimisation purposes, the drag coefficient in heave C_{d_3} is represented as a function of the buoy aspect ratio (H/a) based on data from [22], see Fig. 4. So $C_{d_3} = -0.12(H/a) + 1.2$, while for other motion modes, drag coefficients are kept fixed regardless of the cylinder aspect ratio: $C_{d_1} = C_{d_2} = 1$ for surge and sway, and $C_{d_4} = C_{d_5} = 0.2$ for roll and pitch.

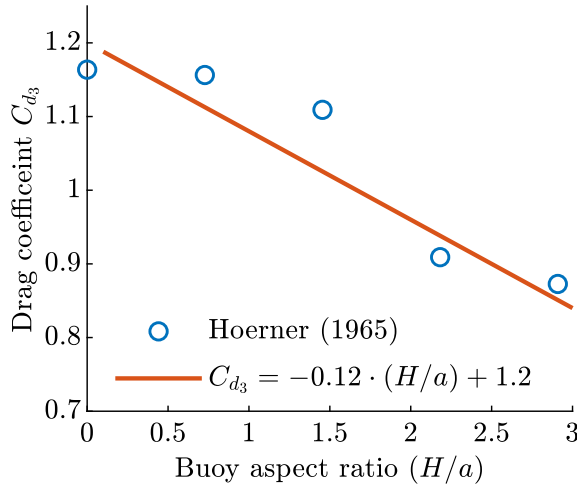


Figure 4: Drag coefficient of the cylindrical body in axial flow as a function of its aspect ratio H/a .

Approximation of LCoE value

Due to the lack of commercial wave power plants, the calculations of the actual LCoE value are based on many uncertainties associated with power production and related costs. [23] assessed various techno-economic related metrics and made a conclusion, that for the CorPower device LCoE can be approximated by the following equation:

$$\text{LCOE} \left(\frac{\text{€}}{\text{kWh}} \right) = \text{RDC} \times \left(\frac{\text{Energy (MWh)}}{\text{Mass (kg)}} \right)^{-0.5}, \quad (15)$$

where the mass corresponds to a significant mass of the WEC including the mass of the buoy and the anchoring system, and RDC is a site-dependent coefficient that will be omitted in calculations (RDC = 1) because optimisation is done for the same deployment site.

In this study, the calculation of the significant mass of the WEC is based on the following assumptions:

- the buoy mass is $m_b = 0.5\rho_w\pi a^2 H$;
- the required mass of the anchoring system (three piles) depends on the tether tension associated with buoyancy and the wave force. Therefore, it can be approximated by:

$$m_{as} = \frac{m_{as}^{\text{ref}}}{(F_t^{\text{peak}})^{\text{ref}}} F_t^{\text{peak}}, \quad (16)$$

where a three-tether WEC with a $a = 5.5$ m radius and $H = 5.5$ m height is taken as a reference case from [18] (the mass of three piles is estimated as $m_{as}^{\text{ref}} = 225 \times 10^3$ kg, and the statistical peak force is $(F_t^{\text{peak}})^{\text{ref}} = 1.94$ MN). Therefore, in order to estimate m_{as} for any given cylinder dimensions, it is required to calculate the tether peak force ($99\% = 2.57\sigma_{F_t}$) using the spectral domain model.

As a result, the LCoE model used in this study is:

$$\text{LCOE} = \left(\frac{8760 P_{AAP}}{m_b + m_{as}} \right)^{-0.5}. \quad (17)$$

OPTIMISATION ROUTINE

Objective functions

The parameters of the WEC that are considered for optimisation are: the buoy radius a , the buoy aspect ratio defined as the ratio of the buoy height to its radius (H/a), the tether inclination angle α_t , the tether attachment angle α_{ap} , the vector of PTO stiffness coefficients for each of the $N = 34$ sea state considered $\mathbf{k}_{pto} = [K_{pto}^{(1)}, K_{pto}^{(2)}, \dots, K_{pto}^{(N)}]^T$, the vector of PTO damping coefficients $\mathbf{b}_{pto} = [B_{pto}^{(1)}, B_{pto}^{(2)}, \dots, B_{pto}^{(N)}]^T$. In total, there are 72 parameters that should be optimised:

$$\mathbf{z} = [a, (H/a), \alpha_t, \alpha_{ap}, \mathbf{k}_{pto} \in \mathbb{R}^{N \times 1}, \mathbf{b}_{pto} \in \mathbb{R}^{N \times 1}]. \quad (18)$$

The two objective functions considered in this study are:

- (i) maximise average annual power output calculated using Eq. (14):

$$f_{O1} = \arg \max_{\mathbf{z}} P_{AAP}(\mathbf{z}), \text{ subject to: } \mathbf{z} \in [\mathbf{z}_{\min}, \mathbf{z}_{\max}] \quad (19)$$

- (ii) minimise LCoE value specified in Eq. (17):

$$f_{O2} = \arg \min_{\mathbf{z}} \text{LCOE}(\mathbf{z}), \text{ subject to: } \mathbf{z} \in [\mathbf{z}_{\min}, \mathbf{z}_{\max}] \quad (20)$$

The range of the design and PTO parameters used in optimisation is specified in Table 1.

Table 1: Constraints on the design parameters.

Parameter	Unit	Min	Max
Buoy radius, a	m	5	20
Buoy aspect ratio, (H/a)		0.4	1.5
Tether inclination angle, α_t	deg	10	80
Tether attachment angle, α_{ap}	deg	10	80
PTO stiffness, K_{pto}	N/m	10^3	10^8
PTO damping, B_{pto}	N/(m/s)	10^3	10^8

Optimisation methods

All methods that we consider are iterative, heuristic approaches, because we do not have a closed mathematical form that might make the optimisation amenable to efficient, purely mathematical optimisation. We employ a range of structurally different methods, not only with the goal of comparing their performance, but also in order to mitigate the inherent search bias that each heuristic has. The latter has the advantage that potentially different locally optimal designs can be compared.

The six methods that we evaluate are:

1. Nelder-Mead (NM) [24], which is a deterministic hill-climber for problems where derivatives are unknown;
2. a simple evolutionary algorithm (1+1EA) [25], which is a stochastic hill-climber, and which (in each iteration) mutates each parameter of a WEC design with a probability of $\frac{1}{\text{number of design variables}}$ using a normal distribution ($\sigma = 0.1 \times (U_b - L_b)$), where U_b and L_b denote the respective variable's upper and lower bound;
3. Particle Swarm Optimisation (PSO) [26], which is a popular heuristic, and which we use with $\lambda = 25$, $c_1 = 1.5$, $c_2 = 2$, $\omega = 1$ (which is exponentially decreased with a damping ratio $w_f = 0.99$);
4. Covariance Matrix Adaptation Evolution Strategy (CMA-ES) [27], which is a state-of-the-art self-adaptive optimiser for continuous spaces, and which we use with the default settings and $\lambda = 16$;
5. Differential Evolution (DE) [28], which is a state-of-the-art method from a different class of algorithms, which employs the concept of crossover to recombine information from other designs, and which we use with a configuration of $\lambda = 25$ (population size), $F = 0.5$ and $P_{cr} = 0.8$;

- SaDE [29], which is a self-adaptive differential evolution. Every one of the strategies/operators in the pool initially has the same probability of being applied. During the evolution, the probabilities are updated based on the number of successfully generated offspring.

Each optimisation run is given a computational budget of 5000 evaluations. As the methods are randomised iterative approaches¹, we repeat each optimisation 10 times.

RESULTS AND DISCUSSION

Objective function f_{O1}

This objective function is related to the maximisation of the annual average power output. The power outputs of the best WEC designs for all six optimisation algorithms are shown as box and whisker plots in Fig. 5. The corresponding optimised design parameters are presented in Table 2.

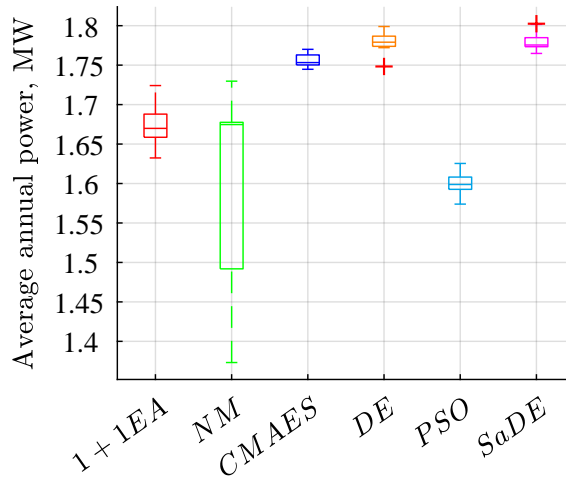


Figure 5: Performance comparison of various optimisation algorithms using objective function f_{O1} (10 independent runs per each method).

Table 2: Optimised design parameters when average annual power is maximised.

Parameter	1+1EA	NM	CMA-ES	DE	PSO	SaDE
a [m]	18.8	18	19.8	19.1	18	19
H/a	1.5	1.49	1.5	1.5	1.5	1.5
α_t [deg]	31	26	28	28	33	26
α_{ap} [deg]	56	55	53	54	53	53
P_{AAP} [MW]	1.72	1.73	1.77	1.77	1.63	1.8

It can be observed that almost all algorithms converged to the configurations with a maximum (or close to) possible radius and height ($a = 18 - 20$ m, $H/a = 1.5$, so $H = 27 - 30$ m), with the highest power output of 1.8 MW produced by SaDE. The radius of the cylinder mainly affects the power absorption properties of the WEC in heave,

¹NM randomly samples the initial WEC designs

while its height affects power from surge. As a result, in order to maximise the power production from each mode of oscillation, a cylindrical WEC should be built as large (and tall) as possible. These results are in agreement with [30], where the power increases with the buoy volume. However, it should be noted that the growth rate of power decreases with the increase in the buoy size, and the cost of manufacturing such large WECs might be not justified by the power generation.

The optimal value of the tether angle α_t depends on the hydrodynamic mode (heave or surge) that is dominant in power production. Thus, for the heaving configuration as $H/a \rightarrow 0$, $\alpha_t \rightarrow 0$ deg (should converge to a single-tether WEC), while for the surging case as $H/a \rightarrow \infty$, $\alpha_t \rightarrow 90$ deg. According to [15], the expected value of α_t for $H/a = 1.5$ should be approximately 52 deg, while all optimisation algorithms provided values $\alpha_t \approx 30$ deg. There might be several reasons for these results. First of all, modelling in [15] has been done using a linear frequency domain model, while in this study the model includes the viscous drag force. Secondly, α_t , α_{ap} , K_{pto} and B_{pto} have a coupled effect on the power generation, and it is possible that there are several combinations of their optimal values that lead to a similar power output.

The optimised values of the tether attachment angle α_{ap} are within a range of 53-56 deg. This angle affects the controllability and power output from pitch motion, so because $\alpha_{ap}^{\text{opt}} > \alpha_t^{\text{opt}}$ the tethers provide better control over pitch. However, we are not aware of any studies on what values should be expected for this cylinder configuration.

As stated above, the optimised designs for this objective function converged to the assigned limits of the cylinder radius and aspect ratio. However, it would be interesting to see how sensitive the power output is to these two parameters. Therefore, for the next set of experiments, values of a and H/a are kept fixed and other parameters are optimised according to the procedure described in Fig. 6. A hybrid optimisation method DE-NM is implemented, where DE (Differential Evolution) is used to optimise the PTO parameters, while NM (Nelder-Mead) is used to optimise the tether angles. Due to the expensive computational cost of these experiments, DE-NM is run only once for each configuration (instead of ten times) in order to visualise the dependence of power on the buoy size.

As a result, Fig. 7 shows the annual average power production of the WEC as a function of its radius and aspect ratio. As expected, the power increases with increasing radius and height. However, a change in radius has a much stronger effect on the power output than a change in height. It is important to note that these results are obtained assuming linear wave theory. However, for such large buoys, the hydrodynamics are most likely nonlinear, and absolute values of power can vary, but the trend is expected to be the same.

Objective function f_{O2}

This objective function is related to the LCoE value approximated as a ratio of the generated energy to the significant mass of the system. The LCoE values for the best geometries obtained by our six optimisation methods are shown in Fig. 8, and the corresponding design parameters are listed in Table 3. Similar to the power maximisation study, all

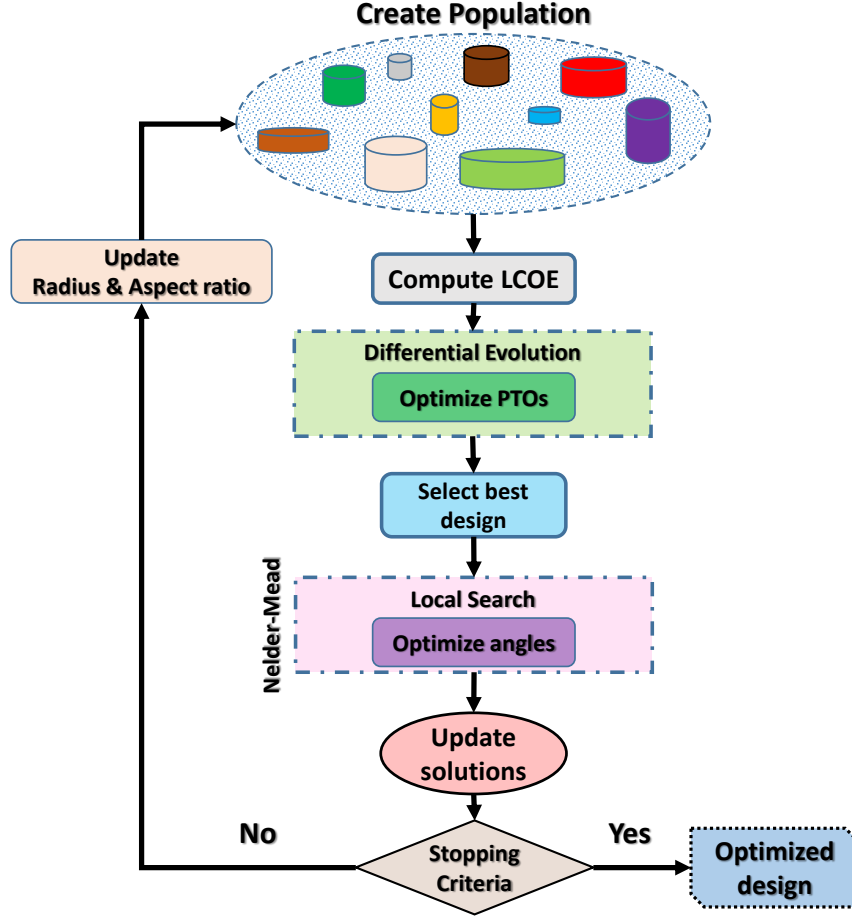


Figure 6: Scheme of proposed hybrid optimisation method (DE-NM).

optimisation algorithms produced similar geometries with SaDE providing the lowest LCoE value. As expected, the WEC design with the lowest LCoE does not have the highest power output and it generates 680 kW.

Table 3: Design parameters when LCoE value is minimised.

Parameter	1+1EA	NM	CMA-ES	DE	PSO	SaDE
a [m]	14.7	14	12.2	12.5	14.1	13
H/a	0.4	0.4	0.4	0.4	0.4	0.4
α_t [deg]	16	17	22	18	21	18
α_{ap} [deg]	10	10	12	10	10	10
LCoE $\times 10^3$	18.5	20.2	20	18.1	20.9	18
Power [MW]	0.7	0.78	0.48	0.61	0.79	0.68

The value of the buoy radius converges to 12-15 m which is very close to the announced design of CETO 6 system with a diameter of 25 m (radius is 12.5 m). This is a very interesting finding as the company run very expensive and accurate CFD simulations to analyse the potential power production, and used a reliable model to estimate the LCoE value. Therefore, it is surprising that the simplistic spectral-domain model with the approximate LCoE calculations generated the same buoy geometry.

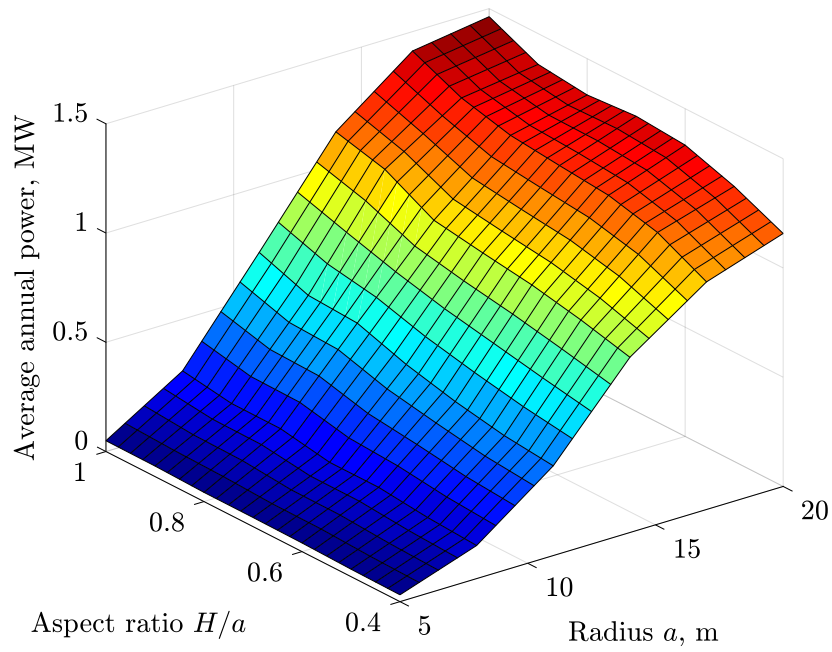


Figure 7: Average annual power output as a function of the buoy radius and aspect ratio obtained using DE-NM.

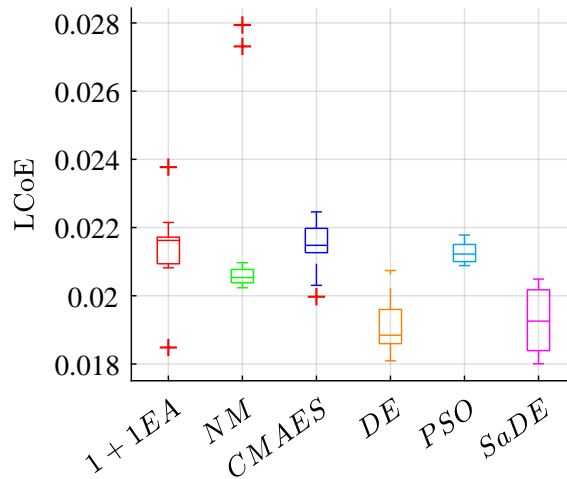


Figure 8: Performance comparison of various optimisation algorithms using objective function f_{O2} (10 independent runs per each method).

In terms of the buoy height, all optimisation algorithms converged to the aspect ratio of 0.4 which is the lower assigned limit for this parameter. So the cylinder should be as short as possible (with a height of 4.8-6 m) in order to generate cheaper energy. A limit of 0.4 is set for the aspect ratio, since there is a possibility to install the power take-off machinery inside the buoy instead of having three independent PTO units on the seabed.

Due to the fact the $H/a \rightarrow 0.4$, the heave mode will be dominant in power production and the optimised tether angle α_t approaches values of 16-22 deg. Such values are also affected by the buoy weight and peak tether forces. So the smaller the tether angle, the less pretension force experienced by tethers and the smaller the mass of the anchoring system. Therefore, it is important to note that the buoy mass can also be included as an optimisation parameter in the future. It is not clear and requires more investigations why the tether attachment angle α_{ap} converged to its lower limit of 10 deg losing controllability over the pitch.

Similar to the power surface plot, the sensitivity of the approximated LCoE value to the buoy design parameters is shown in Fig. 9. It is obvious that energy cost increases with buoy height, while the minimum LCoE can be achieved with a buoy of 11-14 m radius regardless of its height.

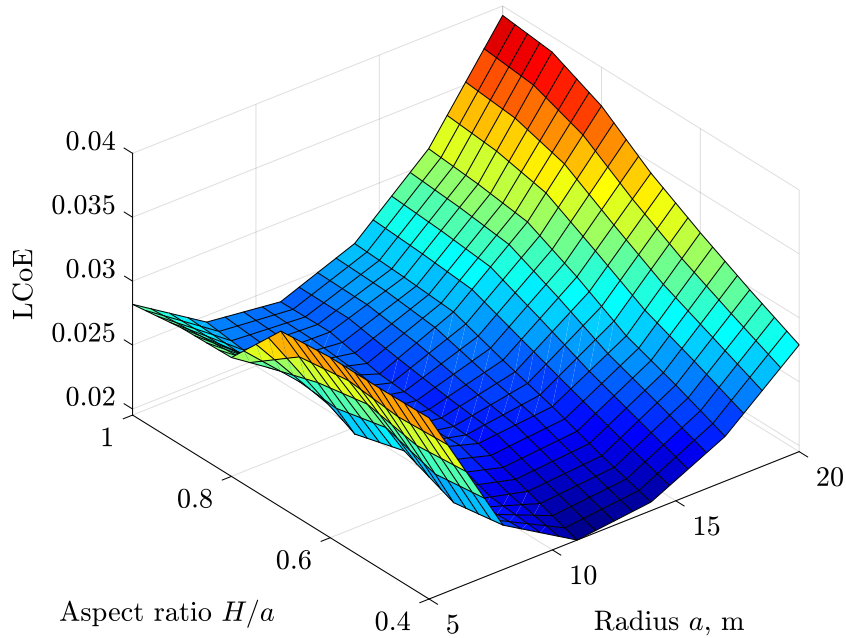


Figure 9: LCoE as a function of the buoy radius and aspect ratio obtained using DE-NM.

For comparison, the best two designs obtained for the two different objective functions are visualised in Fig. 10.

Discussion of optimisation methods

The results discussed so far are those found by the very end of the individual runs of the optimisation approaches. In the following, we briefly present how quickly the algorithms got there. To this end, Figure 11 shows for both objective functions the convergence of the configurations to the final ones.

Across both plots, the trends are largely comparable. DE and SaDE steadily make improvements and eventually perform best. PSO initially performs comparably, but converges quickly. This might be due to the existence of few local optima – note that NM also performs badly in the case of power optimisation – as our previous studies in [31, 32]



Figure 10: The best WEC geometries generated using two different objective functions. Left: power is maximised, right: LCoE value is minimised.

indicated that certain aspects of the problem are unimodal or just bi-modal.² The self-adaptive CMA-ES performs well in the power optimisation scenario, however, it is among the worst performing then considering the LCoE – this might again be explained by the bi-modality: CMA-ES typically works well for multi-modal problems, but the probability of making the jump here (from one corner of the search space to the other) is too small to be performed within only 5000 evaluations. Lastly, what the 1+1EA has in common with the others (except with PSO) is that all algorithms might be able to benefit from a larger computational budget, as all of them have still been making small improvements even after evaluating almost 5000 configurations.

In summary, we conclude that the use of structurally different algorithms allowed us to mitigate the inherent search bias of the respective methods, also because the problem characteristics were not known beforehand. This way, we were able to find good configurations for both the power maximisation and the LCoE minimisation scenarios.

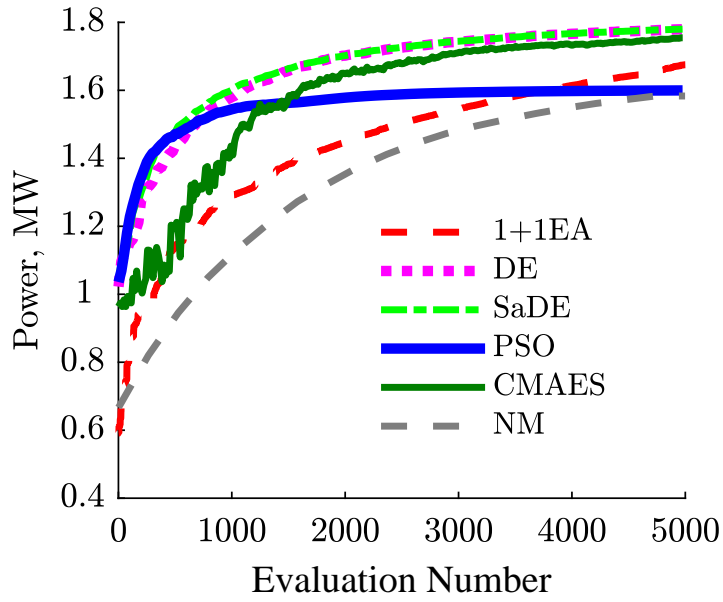
Acknowledgements

Leandro S. P. da Silva acknowledges the Australia-China Science and Research Fund, Australian Department of Industry, Innovation and Science; and the Adelaide Graduate Centre, the University of Adelaide. This work was supported with supercomputing resources provided by the Phoenix HPC service at the University of Adelaide.

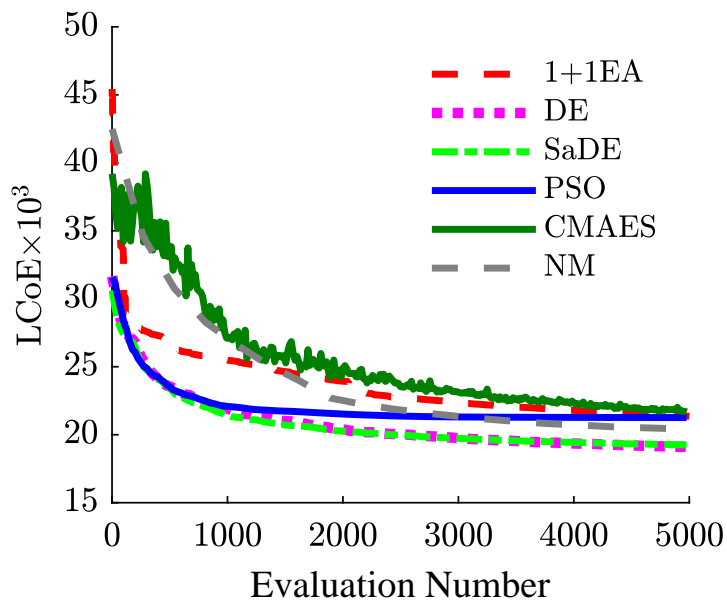
References

- [1] Johannes Falnes and Jorgen Hals. Heaving buoys, point absorbers and arrays. *Philosophical Transactions of the Royal Society A: Mathematical, Physical and Engineering Sciences*, 370(1959):246–277, 2012.

²This means that there are either one or two local optima.



(a)



(b)

Figure 11: Quality of configurations found over time using objective functions (a) f_{O1} , and (b) f_{O2} .

- [2] Jørgen Hals Todalshaug. Practical limits to the power that can be captured from ocean waves by oscillating bodies. *International Journal of Marine Energy*, 3-4(2013):e70–e81, 2013.
- [3] Jørgen Hals Todalshaug. *Hydrodynamics of WECs*, pages 139–158. Springer International Publishing, Cham, 2017.
- [4] Paula B Garcia-Rosa, Giorgio Bacelli, and John V Ringwood. Control-informed geometric optimization of wave energy converters: The impact of device motion and force constraints. *Energies*, 8(12):13672–13687, 2015.
- [5] Yadong Wen, Weijun Wang, Hua Liu, Longbo Mao, Hongju Mi, Wenqiang Wang, and Guoping Zhang. A shape optimization method of a specified point absorber wave energy converter for the south china sea. *Energies*, 11(10):2645, 2018.
- [6] Rezvan Alamian, Rouzbeh Shafaghat, and Mohammad Reza Safaei. Multi-objective optimization of a pitch point absorber wave energy converter. *Water*, 11(5):969, 2019.
- [7] Soheil Esmailzadeh and Mohammad-Reza Alam. Shape optimization of wave energy converters for broadband directional incident waves. *Ocean Engineering*, 174:186–200, 2019.
- [8] LiGuo Wang and John V Ringwood. Geometric optimization of a hinge-barge wave energy converter. In *Proceedings of the 13th European Wave and Tidal Energy Conference*, page 1389, 2019.
- [9] Arthur Pecher and Jens Peter Kofoed. *Handbook of Ocean Wave Energy*. Ocean Engineering & Oceanography. Springer International Publishing, 2017.
- [10] AP McCabe. Constrained optimization of the shape of a wave energy collector by genetic algorithm. *Renewable energy*, 51:274–284, 2013.
- [11] A Garcia-Teruel, D. I. M. Forehand, and Henry Jeffrey. Metrics for wave energy converter hull geometry optimisation. In *Proceedings of the 13th European Wave and Tidal Energy Conference*. EWTEC, 2019.
- [12] Caitlyn E. Clark and Bryony DuPont. Reliability-based design optimization in offshore renewable energy systems. *Renewable and Sustainable Energy Reviews*, 97:390–400, 2018.
- [13] Caitlyn Clark, Anna Garcia-Teruel, Bryony DuPont, and David Forehand. Towards reliability-based geometry optimization of a point-absorber with pto reliability objectives. In *Proceedings of the 13th European Wave and Tidal Energy Conference*, pages 1365–1 – 1365–10, 2019.
- [14] A Garcia-Teruel, D. I. M. Forehand, and Henry Jeffrey. Wave energy converter hull design for manufacturability and reduced lcoe. In *Proceedings of the 7th International Conference on Ocean Energy*, pages 1–9. ICOE2018, 2019.
- [15] N. Y. Sergiienko, B. S. Cazzolato, B. Ding, and M. Arjomandi. An optimal arrangement of mooring lines for the three-tether submerged point-absorbing wave energy converter. *Renewable Energy*, 93:27–37, 2016.
- [16] Australian Wave Energy Atlas, 2017. Accessed 24 October 2017.

- [17] J. T. Scruggs, S. M. Lattanzio, A. A. Taflanidis, and I. L. Cassidy. Optimal causal control of a wave energy converter in a random sea. *Applied Ocean Research*, 42(2013):1–15, 2013.
- [18] N. Y. Sergiienko, A. Rafiee, B. S. Cazzolato, B. Ding, and M. Arjomandi. Feasibility study of the three-tether axisymmetric wave energy converter. *Ocean Engineering*, 150:221–233, 2018.
- [19] N.Y. Sergiienko, B.S. Cazzolato, M. Arjomandi, B. Ding, and L.S.P. da Silva. Considerations on the control design for a three-tether wave energy converter. *Ocean Engineering*, 183:469 – 477, 2019.
- [20] Matt Folley. *Numerical modelling of wave energy converters: State-of-the-art techniques for single devices and arrays*. Elsevier Science, Saint Louis, 2016.
- [21] L.S.P. Silva, N.Y. Sergiienko, C.P. Pesce, B. Ding, B. Cazzolato, and H.M. Morishita. Stochastic analysis of nonlinear wave energy converters via statistical linearization. *Applied Ocean Research*, 95:102023, 2020.
- [22] S.F. Hoerner. *Fluid-dynamic drag: Practical information on aerodynamic drag and hydrodynamic resistance*. Hoerner Fluid Dynamics, 1965.
- [23] Adrian De Andres, Jérôme Maillet, Jørgen Hals Todalshaug, Patrik Möller, David Bould, and Henry Jeffrey. Techno-economic related metrics for a wave energy converters feasibility assessment. *Sustainability*, 8(11):1109, 2016.
- [24] Jeffrey C Lagarias, James A Reeds, Margaret H Wright, and Paul E Wright. Convergence properties of the nelder–mead simplex method in low dimensions. *SIAM Journal on optimization*, 9(1):112–147, 1998.
- [25] Aguston Eiben, Zbigniew Michalewicz, Marc Schoenauer, and Jim Smith. Parameter control in evolutionary algorithms. *Parameter setting in evolutionary algorithms*, pages 19–46, 2007.
- [26] Russell Eberhart and James Kennedy. A new optimizer using particle swarm theory. In *Symposium on Micro Machine and Human Science (MHS)*, pages 39–43. IEEE, 1995.
- [27] Nikolaus Hansen. The cma evolution strategy: a comparing review. *Towards a new evolutionary computation*, pages 75–102, 2006.
- [28] Rainer Storn and Kenneth Price. Differential evolution—a simple and efficient heuristic for global optimization over continuous spaces. *Journal of global optimization*, 11(4):341–359, 1997.
- [29] A Kai Qin, Vicky Ling Huang, and Ponnuthurai N Suganthan. Differential evolution algorithm with strategy adaptation for global numerical optimization. *IEEE transactions on Evolutionary Computation*, 13(2):398–417, 2008.
- [30] A Babarit, J Hals, M Muliawan, A Kurniawan, T Moan, and J Krokstad. Numerical estimation of energy delivery from a selection of wave energy converters – final report. Report, Ecole Centrale de Nantes & Norges Teknisk-Naturvitenskapelige Universitet, 2011.

- [31] Mehdi Neshat, Bradley Alexander, Markus Wagner, and Yuanzhong Xia. A detailed comparison of meta-heuristic methods for optimising wave energy converter placements. In *Proceedings of the Genetic and Evolutionary Computation Conference*, pages 1318–1325. ACM, 2018.
- [32] Mehdi Neshat, Bradley Alexander, Nataliia Sergiienko, and Markus Wagner. A hybrid evolutionary algorithm framework for optimising power take off and placements of wave energy converters. *arXiv preprint arXiv:1904.07043*, 2019.